Dyslipidemia, metabolism and autophagy : antigen-independent modulation of T cells in atherosclerosis

Amersfoort, J.

CHAPTER 6

Lipocalin-2 contributes to experimental atherosclerosis in a stage-dependent manner

Atherosclerosis 2018, 275;214-224

J. Amersfoort[1]
F.H. Schaftenaar[1]
H. Douna[1]
P.J. van Santbrink[1]
M.J. Kröner[1]
G.H.M. van Puijvelde[1]
P.H.A. Quax[2,3]
J. Kuiper[1]
I. Bot[1]

[1]Division of Biotherapeutics, LACDR, Leiden University, Einsteinweg 55, 2333CC, Leiden, The Netherlands
[2]Department of Surgery, Leiden University Medical Center, Albinusdreef 2, 2333ZA, Leiden, The Netherlands
[3]Einthoven Laboratory for Experimental Vascular Medicine, Leiden University Medical Center, Leiden, The Netherlands

ABSTRACT

Background

Lipocalin-2 (Lcn2) is a glycoprotein which can be secreted by immune cells. Several studies in humans have suggested Lcn2 can be used as a biomarker for the detection of unstable atherosclerotic lesions, partly as it is known to interact with MMP-9.

Methods

In this study we generated *Ldlr*$^{-/-}$*Lcn2*$^{-/-}$ mice to study the functional role of Lcn2 in different stages of atherosclerosis. Atherosclerotic lesions were characterized through histological analysis and myeloid cell populations were examined using flow cytometry.

Results

We show that *Ldlr*$^{-/-}$*Lcn2*$^{-/-}$ mice developed larger atherosclerotic lesions during earlier stages of atherosclerosis and had increased circulating Ly6C^{hi} inflammatory monocytes compared to *Ldlr*$^{-/-}$ mice. Advanced atherosclerotic lesions from *Ldlr*$^{-/-}$*Lcn2*$^{-/-}$ mice had decreased necrotic core area suggesting Lcn2 deficiency may affect lesion stability. Furthermore, MMP-9 activity was diminished in plaques from *Ldlr*$^{-/-}$*Lcn2*$^{-/-}$ mice.

Conclusion

Altogether, these findings suggest that Lcn2 deficiency promotes lesion growth in earlier stages of the disease while it decreases MMP-9 activity and necrotic core size in advanced atherosclerosis.

KEYWORDS

Atherosclerosis, lipocalin-2, necrotic core, MMP-9, monocytes

INTRODUCTION

The development of atherosclerosis and subsequent atherosclerotic plaque destabilization are the main underlying pathology of (ischemic) heart disease. Therefore, early detection of unstable atherosclerotic plaques using biomarkers could prove useful to reduce the incidence of acute cardiovascular syndromes. A potential candidate to use as a biomarker for unstable atherosclerosis is lipocalin-2 (Lcn2), which is also known as 24p3 in mice and in humans as neutrophil-gelatinase associated lipocalin (NGAL).

Lcn2 is a secreted glycoprotein which was originally identified as a product of human neutrophils [1, 2]. Upon bacterial infection, Lcn2 functions as a bacteriostatic agent by sequestering iron from bacterial siderophores, such as enterobactin [3]. During inflammation, Lcn2 can act as an inflammatory mediator by binding N-formylmethionyl-leucyl-phenylalanine and leukotriene B4 (LTB4) [4]. Interestingly, Lcn2 itself can also act as a chemoattractant for neutrophils during infection [5]. Furthermore, Lcn2 can form a complex with matrix metalloproteinase (MMP)-9, thereby preventing it from being inhibited by tissue inhibitor of metalloproteinases-1 [6]. Active MMP-9 inside atherosclerotic lesions can degrade extracellular matrix and may thus contribute to advanced plaque instability [7, 8]. By stabilizing active MMP-9, Lcn2 may contribute to the degradation of the fibrous cap and destabilization of atherosclerotic plaques in general [9]. In line, several reports suggest that serum NGAL levels can be used to predict the incidence of cardiac events. Serum NGAL levels were for example shown to correlate with levels of C-reactive protein and to predict major adverse cardiac event (MACE) as well as all-cause mortality in patients with a history of CVD [10-12]. Furthermore, serum NGAL/MMP-9 complex levels are associated with MACE in patients 1 year after coronary angiography [13]. Serum NGAL levels were higher in patients with angiographically confirmed coronary artery disease compared to patients without. Additionally, serum NGAL levels were associated with the number of diseased vessels, suggesting serum NGAL levels might be indicative of the severity of disease [14]. Furthermore, patients with symptomatic atherosclerosis in carotid arteries were shown to have higher levels of serum NGAL as compared to asymptomatic patients [15]. mRNA expression of NGAL was also elevated in atherosclerotic plaques of patients with symptomatic carotid atherosclerosis compared to asymptomatic patients [16]. Local NGAL protein levels were also demonstrated to be elevated in unstable versus stable plaques and NGAL content correlated specifically with MMP-9 activity [17]. In mouse models for atherosclerosis, Lcn2 was shown to colocalize with MMP-9 in atherosclerotic plaques [18].

Lcn2 is actually a very pleiotropic protein, as it is also associated with the development of metabolic diseases, which can subsequently contribute to cardiovascular disease [19]. Serum NGAL levels were elevated in obese individuals compared to lean controls and correlated with insulin resistance [20]. Furthermore, NGAL expression was shown to be

elevated in visceral adipose tissue of obese individuals compared to non-obese controls. In adipose tissue, enzymatic activity of NGAL/MMP-9 complexes was increased in obese individuals compared to lean controls [21]. Despite the evidence from literature which suggests that Lcn2 is associated with the development of atherosclerosis and obesity, there are still many questions regarding the exact pathophysiological role for Lcn2 in atherogenesis. Mechanistic insights gained from experimental models studying Lcn2 in multiple stages of atherosclerosis could contribute to the applicability of Lcn2 as a biomarker for early detection of unstable atherosclerosis and coronary artery disease. In this study, we thus aimed to investigate the contribution of Lcn2 to different stages of diet-induced atherosclerosis. We show here that Lcn2 has a stage-dependent contribution to experimental atherosclerosis as it seems to limit lesion development, whereas it potentially contributes to plaque instability in more advanced stages of atherosclerosis.

MATERIALS AND METHODS

Mice

All animal work was performed according to the guidelines of the European Parliament Directive 2010/63EU and the experimental work was approved by the Animal Ethics committee of Leiden University. *Ldlr* deficient (*Ldlr*$^{-/-}$) mice were originally purchased from Jackson Laboratory and further bred in the Gorlaeus Laboratory in Leiden, The Netherlands. Lcn2 deficient (*Lcn2*$^{-/-}$) mice were kindly provided by Dr. Mak [22] and were backcrossed to *Ldlr*$^{-/-}$ mice to generate *Ldlr*$^{-/-}$*Lcn2*$^{-/-}$ mice. The animals were kept under standard laboratory conditions and were fed a normal chow diet and water *ad libitum*, unless otherwise stated.

Microarray on non-constrictive collar-induced carotid atherosclerosis

To determine *Lcn2* gene expression levels during atherosclerotic lesion development, RNA was extracted from atherosclerotic lesions as previously described [23]. In short, *Ldlr*$^{-/-}$ mice were fed a Western-type diet (WTD) (Special Diet Services) two weeks before surgery and throughout the experiment. To determine the gene expression levels in plaques, atherosclerotic carotid artery lesions were induced by perivascular collar placement as described previously [24]. Both common carotid arteries were excised, snap-frozen in liquid nitrogen and stored at −80°C until further use. Three carotid artery segments carrying carotid plaques from 2, 4, 6, 8 or 10 weeks after collar placement (t=2 until t=10) were pooled for each sample and homogenized by grounding in liquid nitrogen with a pestle [25, 26]. Carotid arteries without atherosclerosis from mice which were only fed a WTD for two weeks served as a control (t=0). Per time point we performed a microarray on three pooled samples.

An additional collar-induced atherosclerosis experiment with a similar design was performed in parallel to generate RNA samples for real-time quantitative PCR analysis as described below. In this setup we again pooled three carotids into one sample and generated the following pooled samples per time point: for t=0 (n=4), for t=2,4 or 6 (n=5) for t=8 (n=4) and for t=10 (n=3). In addition we also stored carotids from *Ldlr*$^{-/-}$ mice that had not been fed a Western type diet and these carotids were used to compare with the t=0 time point, which reflects carotids that were in a hyperlipidemic environment but did not contain atherosclerotic plaques. Total RNA was extracted from the tissue homogenates using Trizol reagent according to manufacturer's instructions (Invitrogen). Gene expression profiles were generated using the Illumina Bead-Chip Whole Genome Microarray platform (ServiceXS).

Atherosclerosis

Diet-induced atherosclerosis was established by feeding female *Ldlr*$^{-/-}$ and *Ldlr*$^{-/-}$*Lcn2*$^{-/-}$ mice from 9-12 weeks of age a WTD containing 0.25% cholesterol and 15% cocoa butter (Special Diet Services). Atherosclerosis was induced for either 6 or 12 weeks to study atherosclerotic lesions in an earlier or more advanced stage. At the end-point of the study, the mice were anesthetized by subcutaneous injections with ketamine (100mg/mL), sedazine (25mg/mL) and atropine (0.5mg/mL) after which their vascular system was perfused with PBS at a continuous low flow via heart puncture in the left ventricle. The hearts were collected to examine the atherosclerotic lesions in the aortic root through histological and morphometric analysis.

Histological and morphometric analysis of atherosclerotic lesions

All hearts were embedded in O.C.T. compound (Sakura) and sectioned horizontally to the aortic axis and towards the aortic arch. Upon identification of the aortic root, defined by the trivalve leaflets, 10 µm sections were collected. Mean plaque size (in μm^2) was calculated from five sequential sections, displaying the highest plaque content, using an Oil-red-O staining (Sigma), which stains neutral lipids. Monocytes and macrophages were visualized using a Moma2 antibody (1:1000, Serotec) and an alkaline phosphatase conjugated secondary antibody (1:100, Sigma). To quantify smooth muscle cell content, smooth muscle cells were visualized by an α-smooth muscle cell actin (αSMA) staining (1:1000, Abcam) and a horseradish peroxidase conjugated secondary antibody. Collagen content inside the plaques was quantified using a Mason's Trichrome staining (Sigma). In the same sections, necrotic areas were identified as intimal a-cellular, debris-like areas. Neutrophils were stained for using the naphtol AS-D chloroacetate esterase staining kit (Sigma). Image quantification was performed blinded for genotype using the Leica Image analysis system (Leica Ltd). Apoptotic cells were stained using the In Situ Cell Death Detection Kit (Sigma) per the manufacturer's protocol. On the same sections,

macrophages were stained using a rat-anti-mouse F4/80 antibody (1:100, Biorad) and an Alexa Fluor 647 conjugated goat-anti-rat IgG as a secondary antibody (1:100, Thermo Fisher Scientific). Nuclei were visualized using Fluoroshield mounting medium with DAPI (Sigma). To quantify apoptosis, TUNEL positive nuclei were quantified inside atherosclerotic lesions. To quantify apoptotic macrophages, TUNEL positive nuclei which were colocalized with F4/80 staining were quantified. Quantification of apoptosis was performed using a Nikon TiE 2000 confocal microscope.

In situ zymography

Non-fixed hearts were snapfrozen on dry ice and stored until further use. 10 µm cryosections were acquired from the three-valve area and air dried for 1-2 hours before storage at -80°C. Cryosections were washed in reaction buffer (150 mM NaCl, 5 mM $CaCl_2$, 50 mM Tris-HCl, pH=7.6) and incubated in reaction buffer containing 30 µg/mL DQ-Gelatin (Molecular probes) and 20 mM MMP2-inhibitor OA-Hycis-9-Octadeconoyl-N-hydroxylamide (Merck Millipore) overnight at 37°C. 1 mM 1,10-phenantrolin is an MMP inhibitor and thus served as a control. After incubation, the sections were washed in reaction buffer and subsequently incubated in 0.5% Chicago Sky Blue (Sigma) for 5 min. to dampen autofluorescence. Finally, the slides were mounted in Fluoroshield medium with DAPI (Sigma) and imaged using the Leica Image analysis system (Leica Ltd).

Real-time quantitative PCR

RNA was extracted from mechanically disrupted common carotid arteries or aortic arches by using Trizol reagent according to manufacturer's instructions (Invitrogen) after which cDNA was generated using RevertAid M-MuLV reverse transcriptase per the instructions of the manufacturer (Thermo Scientific). Quantitative gene expression analysis was performed using Power SYBR Green Master Mix on a 7500 Fast Real-Time PCR system (Applied Biosystems). Gene expression was normalized to housekeeping genes (supplementary table 1).

Immunoblot

Atherosclerotic aortic arches were snapfrozen in liquid nitrogen and stored at -80°C until further use. For protein isolation, tissue samples were homogenized by mechanical disruption and lysed with 1xRIPA (Cell Signaling Technology) supplemented with cOmplete™ Protease Inhibitor Cocktail (Sigma) and 0.1% SDS for 1h on ice. Subsequently, the samples were centrifuged for 15 min. at 15,000 rpm at 4°C and the supernatant was harvested. The samples were diluted in NuPAGE™ LDS Sample Buffer (Thermo Fisher Scientific) prior to SDS-PAGE and subsequent transfer to a nitrocellulose membrane. Proteins were detected using rabbit-anti-mouse MMP-9 (1:1000, Abcam) and rabbit-anti-mouse β-actin (1:1000, Novus Biologicals) antibodies.

Flow cytometry

Blood samples and spleens were collected upon sacrifice. Erythrocytes were subsequently lysed using ACK lysis buffer to prepare the leukocyte fraction for staining of surface markers. For analysis of surface markers, cells were stained at 4°C for 30 min. in PBS containing 2% (vol/vol) fetal bovine serum (FBS) with antibodies from eBioscience and BD Biosciences (supplementary table 2). Flow cytometric analysis was performed on a FACSCantoII (BD Biosciences) and data was analyzed using Flowjo software (TreeStar).

Serum analysis

For measurement of blood glucose levels, mice were fasted for 4 hours prior to blood collection. Blood samples were taken from the tail vein and directly applied to an Accu-Check glucometer (Roche Diagnostics). The levels of serum CCL2, insulin and mouse Amyloid A were determined by ELISA according to manufacturer's protocol (CCL2; BD Biosciences, insulin and mouse Amyloid A; Thermo Fisher Scientific). Concentration of total cholesterol in the serum of unfasted mice was determined by an enzymatic colorimetric assay (Roche Dagnostics). Concentration of triglycerides in the serum was determined by an enzymatic colorimetric assay. Precipath (standardized serum, Roche Diagnostics) was used as an internal standard in the measurements for cholesterol and triglycerides.

Statistical analysis

Data are expressed as mean ± SEM. Datasets were examined for outliers using the ROUT method in GraphPad Prism version 7.00. A two-tailed Student's T-test was used to compare individual groups with Gaussian distributed data. Non-parametric data was analyzed using a Mann-Whitney U-test. Data from three or more groups were analyzed using a one-way ANOVA whereas data from three groups with more than one variable were analyzed by a two-way ANOVA, both with a subsequent Sidak multiple comparison test. A p-value below 0.05 was considered significant.

RESULTS

Lcn2 mRNA expression during collar-induced atherosclerosis

To confirm that Lcn2 expression is increased in atherosclerotic carotid arteries as compared to healthy non-atherosclerotic carotid arteries, we assessed *Lcn2* expression levels by performing a microarray on collar-induced atherosclerotic lesions from Western type diet (WTD, 0.25% cholesterol and 15% cacao butter) fed *Ldlr*$^{-/-}$ mice at different time points after collar placement. Herein, carotid arteries from mice which were fed a WTD for 2 weeks but without collar-induced atherosclerosis served as a control (t=0). *Lcn2*

expression is sharply increased two weeks (t2) after collar placement when compared to unaffected carotid arteries (figure 1A). Although not as pronounced, *Lcn2* expression remained elevated as plaque development progresses four to ten weeks after collar placement (figure 1A). In the same experiment, microarray analysis revealed that the expression of the gene encoding the Lcn2 receptor *24p3r* was unaltered during atherosclerosis (figure 1B). RT-qPCR analysis of *Lcn2* expression in atherosclerotic carotid arteries from an additional collar-induced atherosclerosis experiment in *Ldlr*$^{-/-}$ mice confirmed that Lcn2 expression was elevated during collar-induced atherosclerosis especially after 6, 8 and 10 weeks (figure 1C).

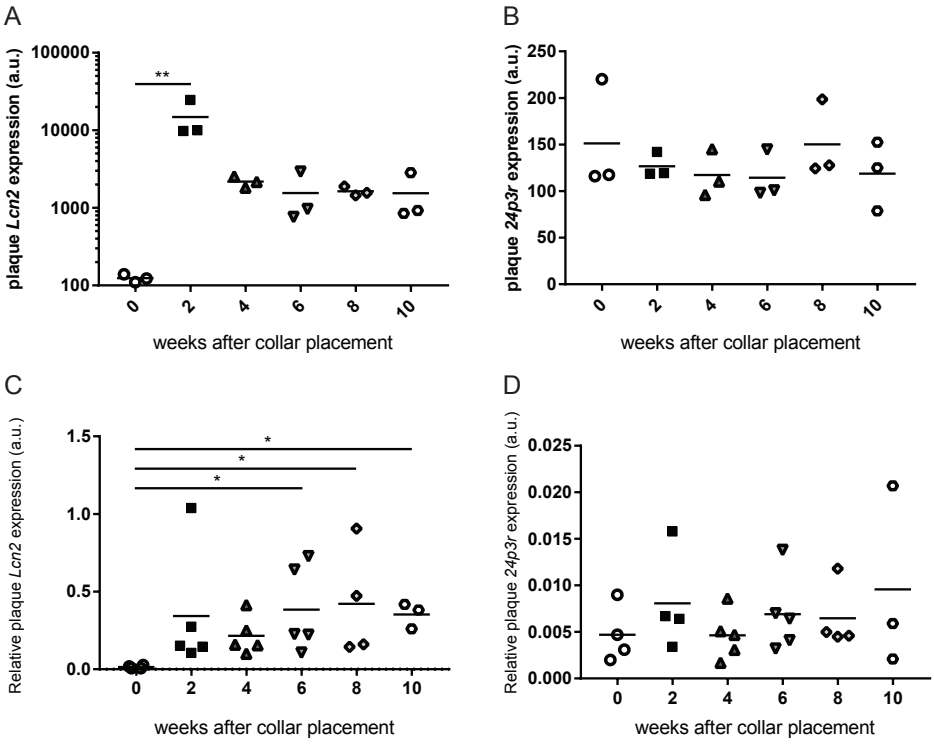

Figure 1 *Lcn2*, but not *24p3r*, mRNA expression was increased in collar-induced atherosclerosis in *Ldlr*$^{-/-}$ mice. (A) A microarray on carotid arteries of *Ldlr*$^{-/-}$ mice without (t=0) or with collar-induced atherosclerosis showed *Lcn2* expression is significantly upregulated 2 weeks after collar placement. Hereafter, it remained elevated from 4 until 10 weeks after collar placement, albeit less pronounced. (B) In the same microarray as in (A), expression of the Lcn2 receptor *24p3r* was unaltered during plaque development. (C) In a parallel collar-induced atherosclerosis experiment, we performed RT-qPCR analysis of *Lcn2* expression in the carotid arteries of mice and *Lcn2* expression was confirmed to be elevated during atherosclerosis. (D) In accordance to (B), RT-qPCR analysis revealed that *24p3r* expression was unaltered during plaque development. n=3 per time point for A-B and n=3-5 for C-D. (*p<0.05, **p<0.01).

Importantly, RT-qPCR analysis of *Lcn2* expression in carotid arteries from *Ldlr*$^{-/-}$ mice which were fed a normal chow diet or a WTD showed that a WTD alone did not induce *Lcn2* expression (median±interquartile range; NCD: 0.0067±0.009 vs WTD: 0.013±0.019, p=0.35). *24p3r* expression was also measured using RT-qPCR and confirmed to be unaltered during atherosclerosis (figure 1D). Thus, atherosclerotic carotid arteries displayed higher levels of *Lcn2* expression as compared to non-atherosclerotic carotid arteries.

Metabolic health status of *Ldlr*$^{-/-}$*Lcn2*$^{-/-}$ mice

To examine the effects of Lcn2 deficiency on atherosclerosis, *Ldlr*$^{-/-}$*Lcn2*$^{-/-}$ and *Ldlr*$^{-/-}$ mice were fed a WTD for 6 or 12 weeks. As Lcn2 is associated with the development of metabolic diseases which can contribute to atherosclerosis (e.g. obesity) various parameters of obesity and insulin resistance were examined. During the experiment, Lcn2 deficiency resulted in a lower body weight after 7 weeks of WTD but otherwise did not result in differences in body weight (figure 2A). Accordingly, inguinal white adipose tissue (iWAT) weight did not differ significantly when comparing *Ldlr*$^{-/-}$*Lcn2*$^{-/-}$ mice to *Ldlr*$^{-/-}$ mice after 6 or 12 weeks of feeding WTD (figure 2B). Total cholesterol levels in serum after 3, 6 or 12 weeks of WTD showed no differences between *Ldlr*$^{-/-}$*Lcn2*$^{-/-}$ mice and *Ldlr*$^{-/-}$ mice (figure 2C). Triglyceride levels in serum after 3, 6 or 12 weeks were also equal between *Ldlr*$^{-/-}$*Lcn2*$^{-/-}$ mice and *Ldlr*$^{-/-}$ mice (figure S1A). Fasting glucose levels were also similar between the groups at these time points (figure 2D). In line, insulin levels were similar between both groups after both 6 and 12 weeks of WTD feeding (figure S1B).

Atherosclerotic plaque formation in *Ldlr*$^{-/-}$*Lcn2*$^{-/-}$ mice

Lcn2 expression in atherosclerotic plaques of aortic arches was increased after 12 weeks WTD compared to 6 weeks WTD in the *Ldlr*$^{-/-}$ group (figure 3A). After 6 weeks of WTD feeding, *Ldlr*$^{-/-}$*Lcn2*$^{-/-}$ mice developed ~20% larger plaques (figure 3B). The intraplaque macrophage content as measured by MOMA2 staining was not significantly altered (figure 3C). Total neutrophil numbers in the plaque and adventitia were not significantly different between both groups (figure 3D). As compared to *Ldlr*$^{-/-}$ mice, *Ldlr*$^{-/-}$*Lcn2*$^{-/-}$ mice had higher intraplaque smooth muscle cell content as measured by αSMA staining (figure 3E). The collagen content in the plaques was equal between the two groups after 6 weeks of WTD (figure 3F). Interestingly, as opposed to the effect on plaque size after 6 weeks of diet feeding, plaque size after prolonged diet feeding was similar in *Ldlr*$^{-/-}$*Lcn2*$^{-/-}$ and *Ldlr*$^{-/-}$ mice after 12 weeks of WTD (figure 3G). Plaques of *Ldlr*$^{-/-}$*Lcn2*$^{-/-}$ did not differ significantly from *Ldlr*$^{-/-}$ mice in terms of MOMA2 staining (figure S2A), total neutrophil numbers (figure S2B), or intraplaque smooth muscle cell percentage (figure S2C) after 12 weeks of WTD. However, a reduction in acellular, necrotic area was observed in advanced atherosclerotic lesions from *Ldlr*$^{-/-}$*Lcn2*$^{-/-}$ mice (figure 3G), which was not the case for atherosclerotic plaques after 6 weeks of WTD feeding (figure S2D). The collagen

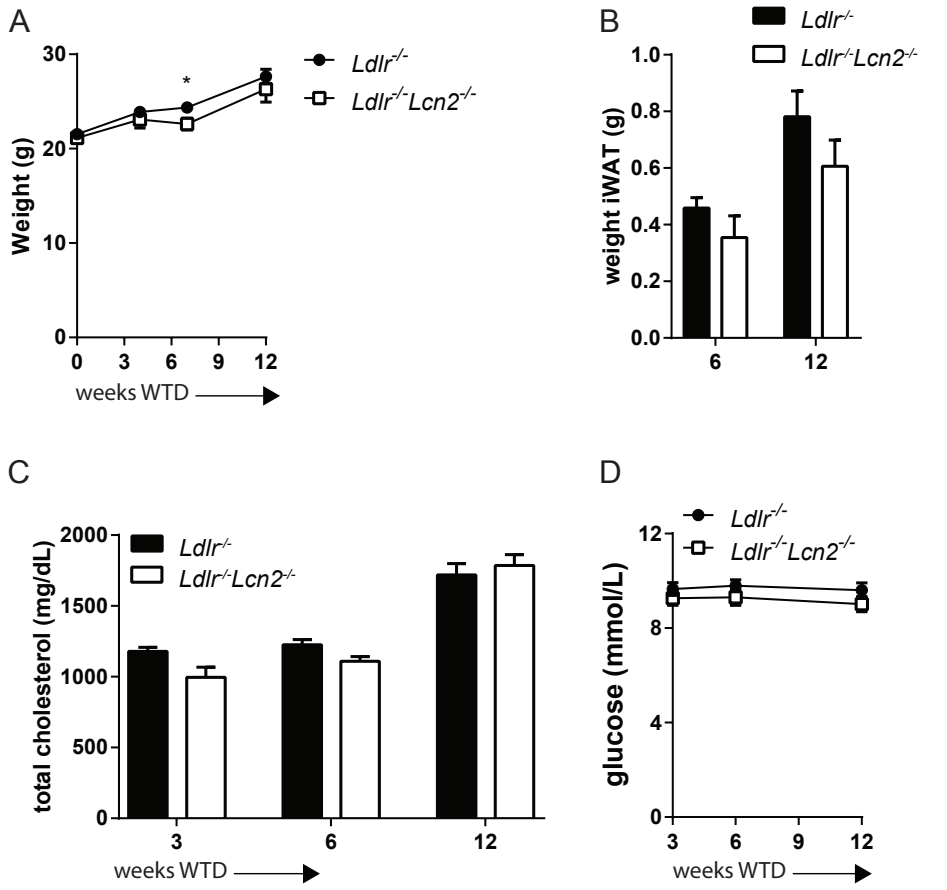

Figure 2 *Ldlr*$^{-/-}$*Lcn2*$^{-/-}$ mice were metabolically similar to *Ldlr*$^{-/-}$ mice (A) *Ldlr*$^{-/-}$*Lcn2*$^{-/-}$ mice showed a significantly higher body weight as compared to *Ldlr*$^{-/-}$ mice after seven weeks of WTD. Otherwise, no differences in weight were observed at different time points (B) In line with this, inguinal white adipose tissue (iWAT) was equal between both groups. (C) Total cholesterol levels in the serum were unaltered between both groups. (D) Fasting glucose was measured over time. No significant changes were observed between the *Ldlr*$^{-/-}$*Lcn2*$^{-/-}$ group and its *Ldlr*$^{-/-}$ controls. n=10-12 per group. All values are depicted as mean±SEM. (*p<0.05).

content in advanced lesions was unaltered when comparing lesions from *Ldlr*$^{-/-}$*Lcn2*$^{-/-}$ to *Ldlr*$^{-/-}$ mice (figure 3H). The percentage of plaque (plaque area/lumen area*100%) was not significantly higher in *Ldlr*$^{-/-}$*Lcn2*$^{-/-}$ mice although it did show a trend towards being higher after 6 (figure S2E) and 12 weeks of WTD (figure S2F), suggesting outward remodeling occurred as a response to atherosclerosis formation.

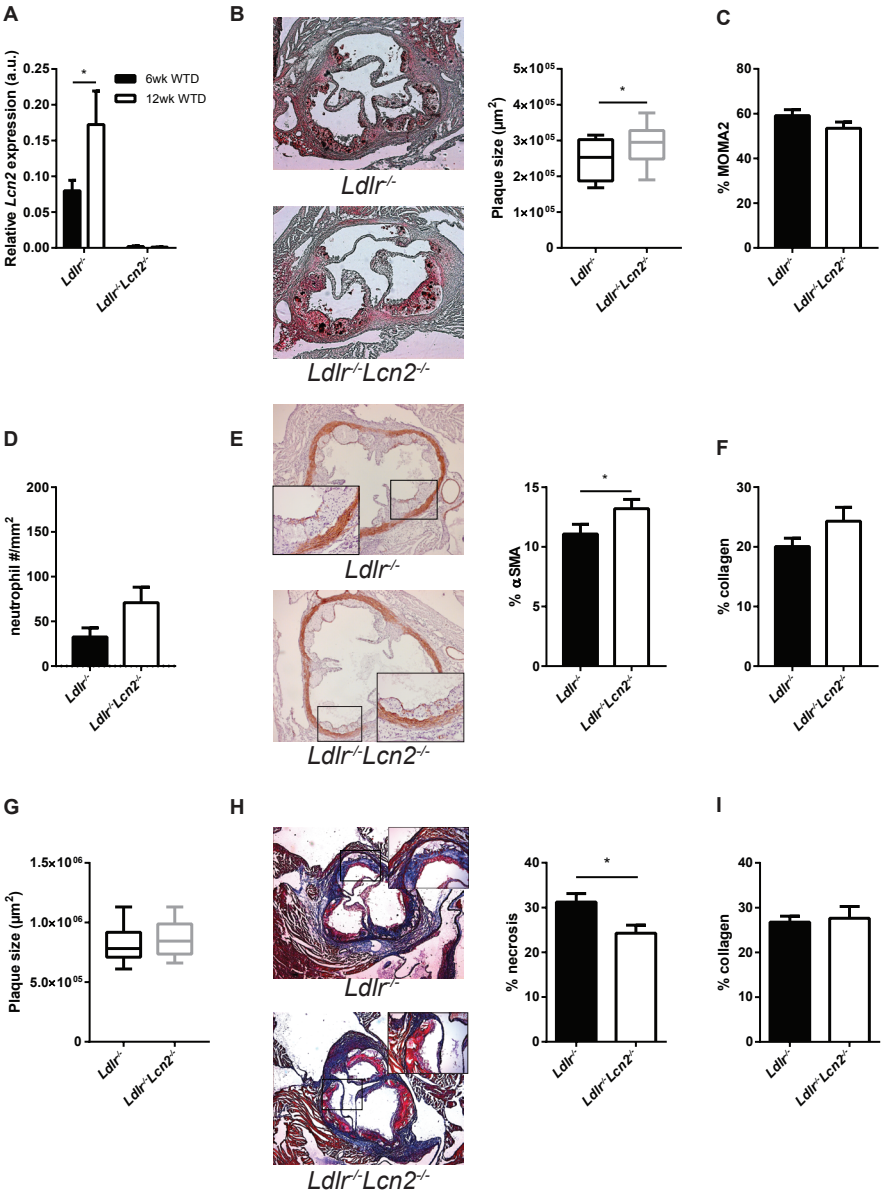

Figure 3 Lcn2 deficiency affected atherosclerosis. (A) *Lcn2* expression in atherosclerotic plaques of aortic arches was increased after 12 weeks WTD compared to 6 weeks WTD in the *Ldlr*$^{-/-}$ group. (B) Lcn2 deficiency resulted in a significant increase in plaque size after 6 weeks WTD. (C) Macrophage content as a percentage of total plaque area measured by MOMA2 staining was unaltered. (D) Neutrophil numbers in the plaque and adventitia showed no difference between both groups. (E) Smooth muscle cell percentage within the lesions was higher in the *Ldlr*$^{-/-}$*Lcn2*$^{-/-}$ group as compared to the controls. (F) Collagen content was equal between both groups. (G) Plaque size of advanced lesions was not significantly different. (H) Necrotic core size was significantly decreased in advanced lesions. (I) Collagen content in advanced lesions was equal between both groups. n=6 per group for (A). n=12 for (B-H). All values are depicted as mean±SEM (*p<0.05).

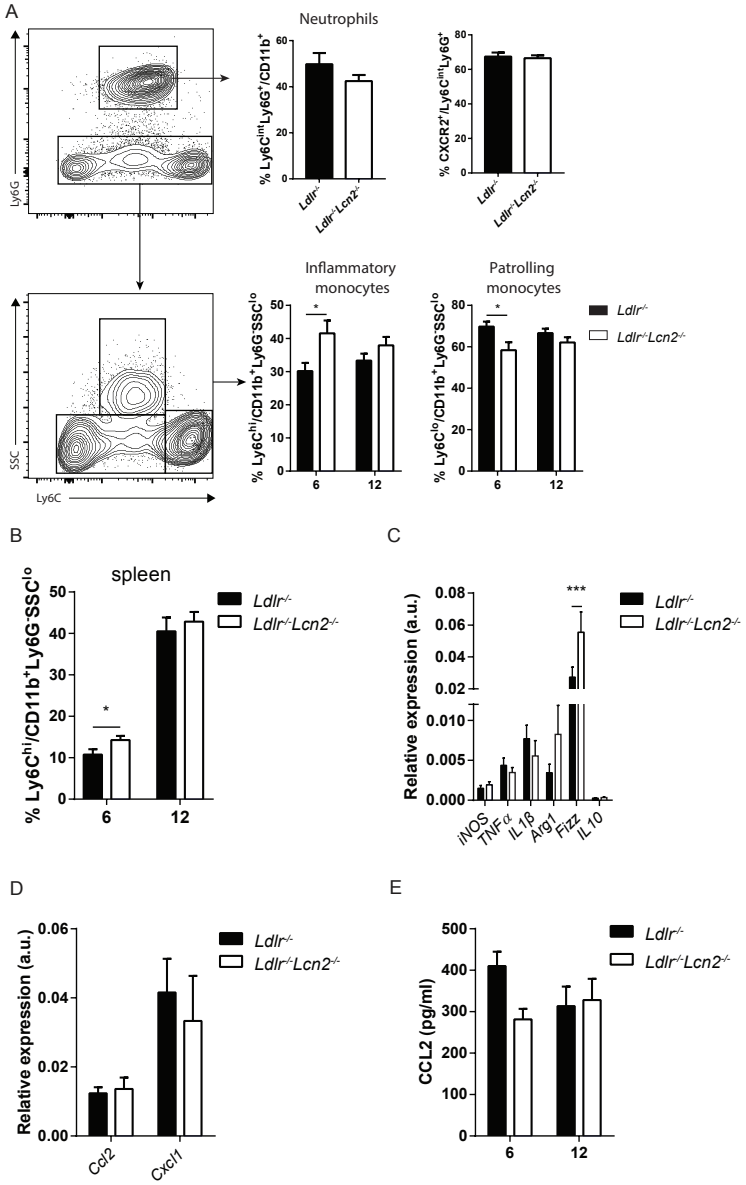

Figure 4 Analysis of myeloid cell populations. (A) The gating strategies for neutrophils, eosinophils and monocytes are depicted. Circulating neutrophil and eosinophil abundance was unaltered. Neutrophils had similar expression levels of the homing receptor CXCR2. Inflammatory monocytes were increased in *Ldlr*$^{-/-}$*Lcn2*$^{-/-}$ mice after 6 weeks of WTD with concomitant decreases in patrolling monocytes. (B) The splenic inflammatory monocyte population showed a similar increase in *Ldlr*$^{-/-}$*Lcn2*$^{-/-}$ mice. (C) mRNA expression of the M2 macrophage marker Fizz was elevated in the atherosclerotic arch of *Ldlr*$^{-/-}$*Lcn2*$^{-/-}$ mice as compared to *Ldlr*$^{-/-}$ mice (D) mRNA expression of CCL2 and CXCL1 were unaltered in the atherosclerotic aortic arch. (E) No significant differences were observed in serum CCL2 levels between both groups. n=6 per group. All values are depicted as mean±SEM (*p<0.05, **p<0.01, ***p<0.001).

Effects of Lcn2 deficiency on the myeloid cell populations during atherosclerosis

To establish whether Lcn2 deficiency has any effects on the myeloid cell populations during atherosclerosis, flow cytometry on blood and spleen was performed. In line with our observation that neutrophil numbers were unaltered in the lesions of *Ldlr*$^{-/-}$*Lcn2*$^{-/-}$ mice, no significant changes were observed in circulating neutrophils after 6 weeks of WTD, neither in percentages nor in the C-X-C chemokine receptor type 2 (CXCR2)$^{+}$ subset (figure 4A). No significant changes in percentage of eosinophils, as defined as CD11b^{+}Ly6G^{-}Ly6C^{int}SSC^{hi} cells, between both groups was observed (figure S3A). The same results were obtained after 12 weeks of WTD (figure S3B). Interestingly, a higher percentage of circulating Ly6C^{hi} inflammatory monocytes was measured after 6 weeks of WTD. Inflammatory monocytes followed a similar trend after 12 weeks of WTD. Ly6C^{lo} patrolling monocytes were decreased accordingly after 6 weeks, although this did not reach significance after 12 weeks of WTD (figure 4A). No significant changes in myeloid cell or lymphocyte populations were observed in the bone marrow compartment or draining lymph node of the aortic root (data not shown). Together, these data indicate that the circulating monocytes are skewed towards a pro-inflammatory phenotype in the *Ldlr*$^{-/-}$*Lcn2*$^{-/-}$ mice. Although not as pronounced as in the blood, splenic monocytes were significantly elevated as well after 6 weeks WTD (figure 4B). Interestingly, serum amyloid A levels in *Ldlr*$^{-/-}$*Lcn2*$^{-/-}$ mice were higher as compared to *Ldlr*$^{-/-}$ mice after 6 and 12 weeks of WTD (figure S3C) indicating that Lcn2 deficiency alters the inflammatory status during atherogenesis. To examine whether a relative increase in inflammatory monocytes resulted in an increase in M1-like macrophages in the plaque the mRNA expression of M1 markers (*iNOS, TNFα, IL1β*) and M2 markers (*Arg1, Fizz, IL10*) was measured. Lcn2 deficiency had no effect on the expression of *iNOS*, *TNFα* and *IL1β*. Of the M2 markers, only *Fizz* was elevated in the atherosclerotic aortic arch after 12 weeks of WTD (figure 4C). Similarly, after 6 weeks of WTD, Lcn2 deficiency resulted in increased *Fizz* expression in the aortic arch while other M1 and M2 macrophage markers were unaltered (figure S3D). Expression of *CCL2*, a well-recognized chemoattractant for inflammatory monocytes which is also known as MCP-1, was measured in atherosclerotic aortic arches to examine whether increased monocyte recruitment was induced by local expression of CCL2. The expression of CXCL1 (the mouse homologue of IL-8), an important chemoattractant for CXCR2^{+} neutrophils, was measured to confirm that neutrophil recruitment to atherosclerotic lesions was unaltered in *Ldlr*$^{-/-}$*Lcn2*$^{-/-}$ mice. mRNA expression of *CCL2* and *CXCL1* were unaltered in the atherosclerotic aortic arch (figure 4D). No significant changes were observed in CCL2 levels in the serum when comparing *Ldlr*$^{-/-}$*Lcn2*$^{-/-}$ mice to *Ldlr*$^{-/-}$ at the 6 or 12 week time points (figure 4E).

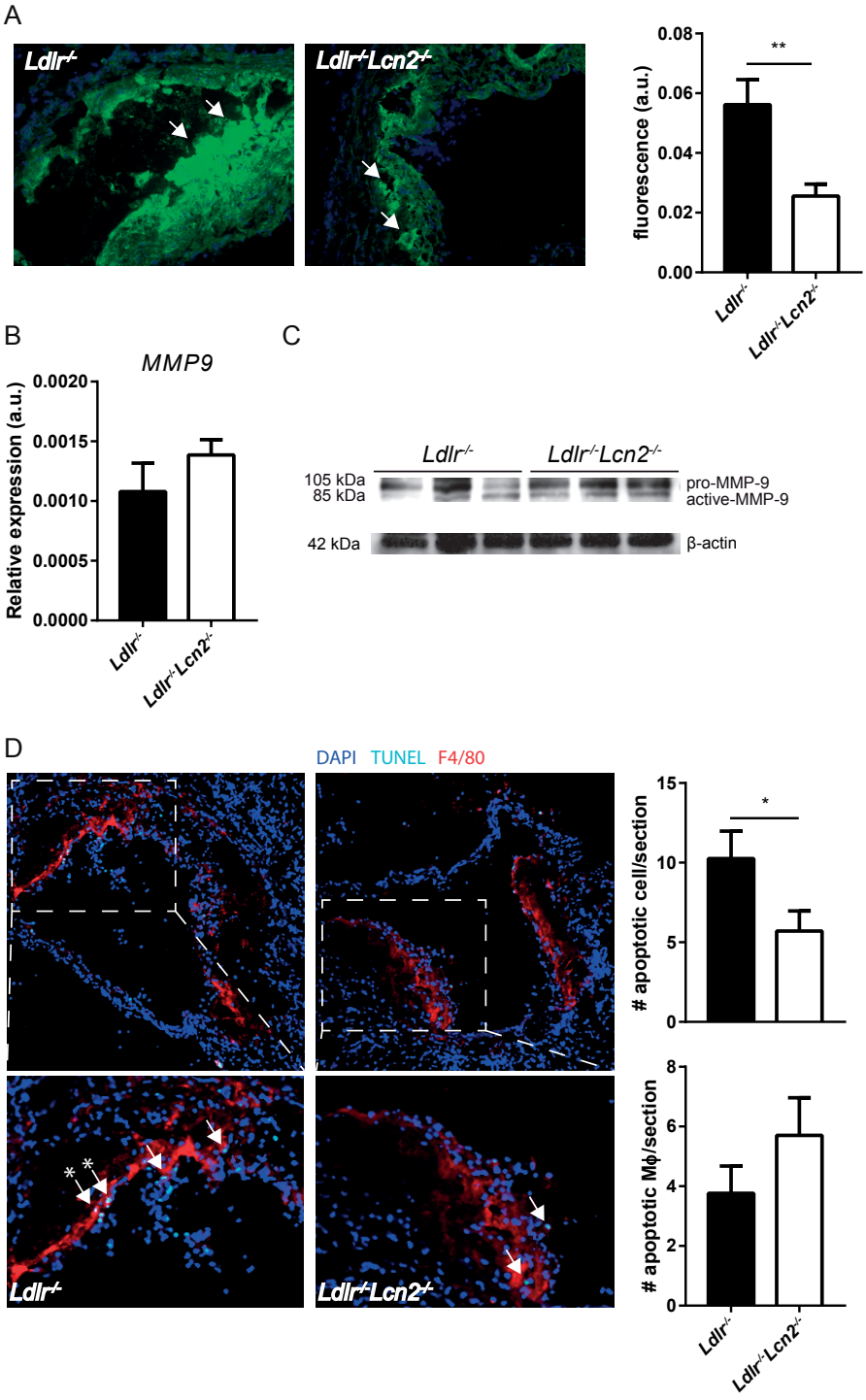
A
Ldlr-/-
Ldlr-/-Lcn2-/-
fluorescence (a.u.)
0.08
0.06
0.04
0.02
0.00
**
Ldlr-/-
Ldlr-/-Lcn2-/-
B
MMP9
Relative expression (a.u.)
0.0020
0.0015
0.0010
0.0005
0.0000
Ldlr-/-
Ldlr-/-Lcn2-/-
C
Ldlr-/-
Ldlr-/-Lcn2-/-
105 kDa
85 kDa
pro-MMP-9
active-MMP-9
42 kDa
β-actin
D
DAPI TUNEL F4/80
Ldlr-/-
Ldlr-/-Lcn2-/-
apoptotic cell/section
15
10
5
0
*
apoptotic Mφ/section
8
6
4
2
0
Ldlr-/-
Ldlr-/-Lcn2-/-

Figure 5 Assessment of MMP-9 activity in atherosclerotic plaques. (A) MMP-9 activity in the aortic root as measured by an in situ zymography was decreased in mice deficient for Lcn2. (B) MMP-9 gene expression in atherosclerotic lesions of the aortic arch was equal between both groups. (C) Similarly, protein expression of MMP-9 was similar between both groups. (D) Lesions from *Ldlr*$^{-/-}$*Lcn2*$^{-/-}$ mice contained fewer apoptotic cells per section but not fewer apoptotic macrophages (MΦ) as compared to lesions from *Ldlr*$^{-/-}$ mice. In (A), gelatinolytic activity is visualized in green and nuclei are stained in dark blue. The white arrows indicate regions with high enzymatic activity. In (D), TUNEL positive nuclei of apoptotic cells are depicted in light blue (indicated with a white arrow) and TUNEL positive nuclei of apoptotic macrophages are depicted in white (indicated with a white arrow and asterisk). Macrophage positive area is depicted in red and nuclei in dark blue. The data in (A) is representative of two experiments. n=10 for figure 5A and 5C. n=6 for figure 5B. All values are depicted as mean±SEM (*p<0.05, **p<0.01).

MMP-9 activity in the aortic root

As a decreased necrotic core size in advanced atherosclerosis could be due to decreased intraplaque proteolytic activity an *in situ* zymography was performed to measure MMP-9 activity in atherosclerotic lesions in the aortic root. An MMP-2 inhibitor was added in the reaction mix to ensure that DQ-gelatin degradation was mainly MMP-9 mediated although some residual signal from other MMPs with gelatinolytic activity may be present. A significant decrease in gelatinolytic activity, a measure for MMP activity, was observed in the *Ldlr*$^{-/-}$*Lcn2*$^{-/-}$ group compared to the control group (Fig 5A). *MMP-9* mRNA expression in the atherosclerotic aortic arch was not significantly different in *Ldlr*$^{-/-}$*Lcn2*$^{-/-}$ mice compared to controls, suggesting that the effects are primarily caused by MMP-9 protein stabilization in the *Ldlr*$^{-/-}$ mice (figure 5B). Immunoblot analysis also showed that MMP-9 protein expression was equal between *Ldlr*$^{-/-}$ and *Ldlr*$^{-/-}$*Lcn2*$^{-/-}$ mice (figure 5C) and quantification of the blot confirmed this (figure S4A). Furthermore, the ratio between the pro- and active form of the MMP-9 protein was unaltered between both genotypes (figure S4B). Interestingly, no differences in *MMP-2* mRNA expression (figure S4C) or *MMP-14* mRNA expression (figure S4D) in the atherosclerotic aortic arches were observed when comparing *Ldlr*$^{-/-}$ mice to *Ldlr*$^{-/-}$*Lcn2*$^{-/-}$. In line with a decreased necrotic core size, lesions from *Ldlr*$^{-/-}$*Lcn2*$^{-/-}$ mice contained fewer apoptotic cells. The number of apoptotic macrophages was equal between both genotypes (figure 5D).

DISCUSSION

Several studies reported that the detection of unstable atherosclerotic plaques using Lcn2 could prove useful in the future to reduce the incidence of acute cardiovascular syndromes, however the direct contribution of Lcn2 to atherosclerotic plaque progression remained up to date uninvestigated.

Microarray analysis of non-constrictive collar-induced atherosclerosis showed that local *Lcn2* expression increased during early stages of atherosclerotic lesion development, and remained elevated during plaque progression. As expression of the Lcn2-receptor *24p3r* was unaltered, local Lcn2 effects in atherosclerotic plaques were mainly regulated by regulating the expression of the protein itself or by regulating the influx of myeloid cells expressing Lcn2, such as neutrophils and monocytes. Based on these findings we studied the effect of Lcn2 deficiency on different stages of atherosclerosis and related this to changes in myeloid cell populations. After 6 weeks of WTD, lesions from *Ldlr*$^{-/-}$*Lcn2*$^{-/-}$ were somewhat larger and had a higher smooth muscle cell percentage as compared to those of *Ldlr*$^{-/-}$ control mice, but plaque composition remained otherwise unaltered. Interestingly, Lcn2 deficiency did not affect advanced lesion size but did display a decrease in necrotic area.

The effects observed on plaque size could not be explained by increased hepatic steatosis and resulting increases in circulating cholesterol levels. A study by Ye et al. described Lcn2 to exert pro-inflammatory effects in a high fat, high cholesterol diet induced model of non-alcoholic steatohepatitis (NASH) [27]. Lcn2 deficiency in mice attenuated the transition of hepatic steatosis to NASH whereas administration of recombinant Lcn2 exacerbated disease in a neutrophil-dependent manner. In the present study, *Ldlr*$^{-/-}$*Lcn2*$^{-/-}$ mice showed no differences in total serum cholesterol or circulating neutrophils which makes it unlikely that hepatic steatosis contributed to the observed lesion effects. *Ldlr*$^{-/-}$*Lcn2*$^{-/-}$ mice were fed a WTD to study atherosclerosis, while a high fat high cholesterol diet was used to study NASH. Presumably, the fact that this diet contains 40% fat and was fed to the mice for 12 to 20 weeks to induce NASH explains why Lcn2 deficiency did not affect the development of hepatic steatosis in the present study.

In this study, Lcn2 deficiency had no effects on body weight or iWAT weight. Feeding a high fat diet to C57BL/6 mice has previously been shown to increase Lcn2 expression by adipocytes and to increase its abundance in serum [28]. These increases are even more pronounced in iWAT compared to epididymal WAT [29]. Furthermore, Lcn2 expression by adipocytes is induced by various pro-inflammatory cytokines which are known to play a role in obesity development, including TNFα, IL1-β and IL-6 [30]. Interestingly, Lcn2 deficient mice which are fed a high fat diet gain more weight compared to wildtype mice [29]. These effects were not observed in our study, possibly due to the fact that our study used female mice whereas most studies on the role of Lcn2 in obesity were performed

in male mice. Additionally, feeding a WTD for 6 or 12 weeks might not have induced a severe enough obese phenotype to observe differences between Lcn2 wildtype or Lcn2 deficient mice. LDLr deficient mice develop hyperglycemia and insulin resistance after approximately 20 weeks of feeding them a WTD [31] and Lcn2 has been shown to affect insulin resistance [19]. The fact that fasting glucose levels were equal between *Ldlr*$^{-/-}$and *Ldlr*$^{-/-}$*Lcn2*$^{-/-}$ mice suggest that in the present study the time frame was too limited to induce obesity and insulin resistance. As the metabolic parameters we examined did not differ between both genotypes it is improbable that atherosclerosis was affected by altered metabolic disease development in *Ldlr*$^{-/-}$*Lcn2*$^{-/-}$ mice.

After 6 weeks of WTD, lesions in *Ldlr*$^{-/-}$*Lcn2*$^{-/-}$ mice were slightly larger compared to *Ldlr*$^{-/-}$ control mice. This finding was rather counterintuitive as Lcn2 is generally considered to be secreted under and promote inflammatory conditions [19]. Interestingly, there are actually also multiple studies describing Lcn2 to be protective in a number of inflammatory diseases. Lcn2 deficient mice have for example increased liver damage in various models for liver injury with concomitant increases in expression of pro-inflammatory factors such as *CCL2, TNFα* and a decrease in *IL-10* expression [32]. Additionally, Lcn2 appears to play a protective role in experimental autoimmune encephalomyelitis pathogenesis as Lcn2 deficient mice have higher lesion burden and increased expression of *IFNγ* and *TNFα* inside lesions [33]. In our study, Lcn2 deficiency did not affect the expression of *TNFα*, *CCL2* in the atherosclerotic aortic arches, suggesting Lcn2 exerts a protective function in atherogenesis which is distinct from other diseases. Upon Lcn2 deficiency, circulating monocytes were skewed towards a more inflammatory phenotype, which may have driven lesion progression, considering the atherogenic effects inflammatory monocytes have on early lesion development [34]. No differences were however observed in macrophage content of the plaques. When plaques from the aortic arch were analyzed for different M1 and M2 macrophage marker expression, it was shown that only the M2 marker *Fizz* was elevated in Lcn2 deficient mice. The phenotypic effects that Lcn2 has on macrophages appear to be condition-specific as different studies have reported treatment of bone marrow-derived macrophages (BMDM) with Lcn2 to increase expression of M1 markers [35] but also IL-10 production [36]. Furthermore, BMDM from *Lcn2*$^{-/-}$ mice showed a more profound upregulation of *IL-1β* and *iNOS* after lipopolysaccharide stimulation compared to wildtype controls [37] whereas infection of Lcn2 deficient peritoneal macrophages with *Salmonella Typhimurium* was reported to result in increased *IL-10* expression as compared to wildtype controls [38]. In the presented study, as Lcn2 can induce foam cell formation in BMDM by inducing the expression of scavenger receptors [35], the absence of Lcn2 might have compensated for increased monocyte homing towards atherosclerotic lesions. It is unclear what causes the increase in monocyte activation. Lcn2 is known to interact with LTB4, which acts as a chemokine for monocytes during development of atherosclerosis [39], but it is unknown what functional consequences this interaction has [4].

The absence of Lcn2 may have increased the potency of LTB4 to activate monocytes, however future studies should shed more light on exact mechanisms involved in Lcn2 mediated monocyte differentiation and migration.

Based on the results, Lcn2 did not function as a chemoattractant for neutrophils to home towards atherosclerotic lesions in this study as neither the number of neutrophils inside the plaques nor the circulating neutrophil percentages were changed. Lcn2 has been shown to serve as a chemoattractant for neutrophils during acute inflammation [5] and during development of NASH by increasing CXCR2-dependent homing towards the liver [27]. Lcn2 deficiency had no effect on *CXCL1* expression in atherosclerotic aortic arches further suggesting Lcn2 deficiency did not alter neutrophil recruitment to atherosclerotic plaques in this study. As compared to Lcn2 levels during acute inflammation, the levels of circulating and local Lcn2 during atherogenesis might not be high enough for Lcn2 deficiency to alter neutrophil recruitment, possibly explaining why Lcn2 deficiency during experimental atherosclerosis had no effect on neutrophil migration.

In advanced atherosclerotic plaques, *Ldlr*$^{-/-}$*Lcn2*$^{-/-}$ mice did show a decreased necrotic core area inside lesions of the aortic root, suggesting that Lcn2 deficiency affected matrix degradation. This was most likely due to the decreased local MMP-9 activity in the Lcn2 deficient mice as measured by zymography. Lcn2 binds to MMP-9 to prevent its inhibition by tissue inhibitor of metalloproteinases [6], leading to more active MMP-9. Proteolytic activity has been shown to induce the apoptosis of macrophages and smooth muscle cells and inhibition of proteolytic activity can decrease necrotic core size accordingly [40-42]. As lesions from Lcn2 deficient mice contained fewer apoptotic cells, a decreased necrotic core size in lesions from Lcn2 deficient mice could be due to a decrease in MMP activity and subsequent proteolysis-induced apoptosis. Previously, Lcn2 and MMP-9 have been shown to colocalize in atherosclerotic lesions [18]. As MMP9 expression inside atherosclerotic lesions of the aortic arch was equal between the *Ldlr*$^{-/-}$*Lcn2*$^{-/-}$ and control groups, the decrease in MMP-9 activity in the Lcn2 deficient mice was unlikely due to decreased MMP-9 abundance, but mainly caused by decreased MMP-9 activity. These findings are in line with literature describing unstable plaques to have higher levels of NGAL than stable plaques [17] and support serum NGAL/MMP-9 complex levels to predict MACE 1 year after follow up [13]. The present study provides evidence that local Lcn2 in advanced stages of atherosclerosis might indeed decrease lesion stability. Whether Lcn2 actually affects lesion stability in advanced atherosclerosis or it only modulates MMP-9 activity and necrotic core size remains to be determined. Nevertheless, our findings suggest that lowering of NGAL levels through therapeutic intervention might be feasible to increase plaque stability in patients with unstable atherosclerosis as the presence of NGAL in advanced atherosclerosis appears to contribute to plaque instability. Interestingly, in patients with carotid artery atherosclerosis, serum NGAL levels were lower in patients on statins as compared to patients without. Also in patients with vulnerable lesions, statin-

treated patients had lower levels of serum NGAL compared to patients without statins [15]. Another study in patients which underwent carotid endarterectomy as a treatment for advanced atherosclerosis showed that serum NGAL levels were equal between patients with or without statin treatment [43]. This suggests that statin treatment can decrease circulating NGAL levels but that this may depend on the patient group which is targeted. There are some limitations to this study. For example, plaque size was determined in the aortic root but not at other sites of lesion development. Another limitation is that we did not perform an oral glucose tolerance test to examine the effects Lcn2 deficiency has on the metabolic health status in these experiments. As this is a highly relevant parameter in assessing the metabolic syndrome-like phenotype diet-induced dyslipidemia can induce, it is not possible to definitely conclude that Lcn2 deficiency had no effects on the metabolic status in our experiments. However, as the total body weight, iWAT weight, fasting glucose and insulin levels in the serum were unaltered between groups it is highly unlikely that Lcn2 deficiency had any effect on the metabolic health status in these experiments. Lastly, in our zymography, other MMPs besides MMP-9 which can degrade gelatin might have caused some background signal. However, areas with high gelatinolytic activity have been shown to colocalize with MMP-9 [18], indicating the gelatinolytic activity which we measured was mainly MMP-9 derived.

In conclusion, Lcn2 deficiency was shown to increase plaque size during earlier stages of lesion development, possibly due to an increase in inflammatory monocytes and without affecting neutrophil recruitment. In addition, this study showed that Lcn2 deficiency decreased the local degree of MMP-9 activity thereby possibly contributing to more stable atherosclerotic plaques. Further studies are required to further examine the effects of Lcn2 on myeloid cell populations during atherogenesis as this might further improve the interpretation of changes in circulating Lcn2 levels.

REFERENCES

1. Kjeldsen, L, Cowland, JB and Borregaard, N, Human neutrophil gelatinase-associated lipocalin and homologous proteins in rat and mouse, Biochim Biophys Acta, 2000;1482:272-283.
2. Kjeldsen, L, Sengelov, H, Lollike, K, et al., Isolation and characterization of gelatinase granules from human neutrophils, Blood, 1994;83:1640-1649.
3. Flo, TH, Smith, KD, Sato, S, et al., Lipocalin 2 mediates an innate immune response to bacterial infection by sequestrating iron, Nature, 2004;432:917-921.
4. Bratt, T, Ohlson, S and Borregaard, N, Interactions between neutrophil gelatinase-associated lipocalin and natural lipophilic ligands, Biochim Biophys Acta, 1999;1472:262-269.
5. Schroll, A, Eller, K, Feistritzer, C, et al., Lipocalin-2 ameliorates granulocyte functionality, Eur J Immunol, 2012;42:3346-3357.
6. Yan, L, Borregaard, N, Kjeldsen, L, et al., The high molecular weight urinary matrix metalloproteinase (MMP) activity is a complex of gelatinase B/MMP-9 and neutrophil gelatinase-associated lipocalin (NGAL). Modulation of MMP-9 activity by NGAL, J Biol Chem, 2001;276:37258-37265.
7. de Nooijer, R, Verkleij, CJ, von der Thusen, JH, et al., Lesional overexpression of matrix metalloproteinase-9 promotes intraplaque hemorrhage in advanced lesions but not at earlier stages of atherogenesis, Arterioscler Thromb Vasc Biol, 2006;26:340-346.
8. Galis, ZS, Sukhova, GK, Lark, MW, et al., Increased expression of matrix metalloproteinases and matrix degrading activity in vulnerable regions of human atherosclerotic plaques, J Clin Invest, 1994;94:2493-2503.
9. Ghattas, A, Griffiths, HR, Devitt, A, et al., Monocytes in coronary artery disease and atherosclerosis: where are we now?, J Am Coll Cardiol, 2013;62:1541-1551.
10. Daniels, LB, Barrett-Connor, E, Clopton, P, et al., Plasma neutrophil gelatinase-associated lipocalin is independently associated with cardiovascular disease and mortality in community-dwelling older adults: The Rancho Bernardo Study, J Am Coll Cardiol, 2012;59:1101-1109.
11. Lindberg, S, Jensen, JS, Hoffmann, S, et al., Plasma Neutrophil Gelatinase-Associated Lipocalin Reflects Both Inflammation and Kidney Function in Patients with Myocardial Infarction, Cardiorenal Med, 2016;6:180-190.
12. Lindberg, S, Pedersen, SH, Mogelvang, R, et al., Prognostic utility of neutrophil gelatinase-associated lipocalin in predicting mortality and cardiovascular events in patients with ST-segment elevation myocardial infarction treated with primary percutaneous coronary intervention, J Am Coll Cardiol, 2012;60:339-345.
13. Cheng, JM, Akkerhuis, KM, Meilhac, O, et al., Circulating osteoglycin and NGAL/MMP9 complex concentrations predict 1-year major adverse cardiovascular events after coronary angiography, Arterioscler Thromb Vasc Biol, 2014;34:1078-1084.
14. Zografos, T, Haliassos, A, Korovesis, S, et al., Association of neutrophil gelatinase-associated lipocalin with the severity of coronary artery disease, Am J Cardiol, 2009;104:917-920.
15. Eilenberg, W, Stojkovic, S, Kaider, A, et al., NGAL and MMP-9/NGAL as biomarkers of plaque vulnerability and targets of statins in patients with carotid atherosclerosis, Clin Chem Lab Med, 2017;56:147-156.
16. Eilenberg, W, Stojkovic, S, Piechota-Polanczyk, A, et al., Neutrophil Gelatinase-Associated Lipocalin (NGAL) is Associated with Symptomatic Carotid Atherosclerosis and Drives Pro-inflammatory State In Vitro, Eur J Vasc Endovasc Surg, 2016;51:623-631.

17. te Boekhorst, BC, Bovens, SM, Hellings, WE, et al., Molecular MRI of murine atherosclerotic plaque targeting NGAL: a protein associated with unstable human plaque characteristics, Cardiovasc Res, 2011;89:680-688.
18. Hemdahl, AL, Gabrielsen, A, Zhu, C, et al., Expression of neutrophil gelatinase-associated lipocalin in atherosclerosis and myocardial infarction, Arterioscler Thromb Vasc Biol, 2006;26:136-142.
19. Moschen, AR, Adolph, TE, Gerner, RR, et al., Lipocalin-2: A Master Mediator of Intestinal and Metabolic Inflammation, Trends Endocrinol Metab, 2017;28:388-397.
20. Wang, Y, Lam, KS, Kraegen, EW, et al., Lipocalin-2 is an inflammatory marker closely associated with obesity, insulin resistance, and hyperglycemia in humans, Clin Chem, 2007;53:34-41.
21. Catalan, V, Gomez-Ambrosi, J, Rodriguez, A, et al., Increased adipose tissue expression of lipocalin-2 in obesity is related to inflammation and matrix metalloproteinase-2 and metalloproteinase-9 activities in humans, J Mol Med (Berl), 2009;87:803-813.
22. Berger, T, Togawa, A, Duncan, GS, et al., Lipocalin 2-deficient mice exhibit increased sensitivity to Escherichia coli infection but not to ischemia-reperfusion injury, Proc Natl Acad Sci U S A, 2006;103:1834-1839.
23. Ackers-Johnson, M, Talasila, A, Sage, AP, et al., Myocardin regulates vascular smooth muscle cell inflammatory activation and disease, Arterioscler Thromb Vasc Biol, 2015;35:817-828.
24. von der Thusen, JH, van Berkel, TJ and Biessen, EA, Induction of rapid atherogenesis by perivascular carotid collar placement in apolipoprotein E-deficient and low-density lipoprotein receptor-deficient mice, Circulation, 2001;103:1164-1170.
25. Bot, M, Bot, I, Lopez-Vales, R, et al., Atherosclerotic lesion progression changes lysophosphatidic acid homeostasis to favor its accumulation, Am J Pathol, 2010;176:3073-3084.
26. Wezel, A, Welten, SM, Razawy, W, et al., Inhibition of MicroRNA-494 Reduces Carotid Artery Atherosclerotic Lesion Development and Increases Plaque Stability, Ann Surg, 2015;262:841-847; discussion 847-848.
27. Ye, D, Yang, K, Zang, S, et al., Lipocalin-2 mediates non-alcoholic steatohepatitis by promoting neutrophil-macrophage crosstalk via the induction of CXCR2, J Hepatol, 2016;65:988-997.
28. Yan, QW, Yang, Q, Mody, N, et al., The adipokine lipocalin 2 is regulated by obesity and promotes insulin resistance, Diabetes, 2007;56:2533-2540.
29. Guo, H, Bazuine, M, Jin, D, et al., Evidence for the regulatory role of lipocalin 2 in high-fat diet-induced adipose tissue remodeling in male mice, Endocrinology, 2013;154:3525-3538.
30. Zhang, Y, Foncea, R, Deis, JA, et al., Lipocalin 2 expression and secretion is highly regulated by metabolic stress, cytokines, and nutrients in adipocytes, PLoS One, 2014;9:e96997.
31. Merat, S, Casanada, F, Sutphin, M, et al., Western-type diets induce insulin resistance and hyperinsulinemia in LDL receptor-deficient mice but do not increase aortic atherosclerosis compared with normoinsulinemic mice in which similar plasma cholesterol levels are achieved by a fructose-rich diet, Arterioscler Thromb Vasc Biol, 1999;19:1223-1230.
32. Borkham-Kamphorst, E, van de Leur, E, Zimmermann, HW, et al., Protective effects of lipocalin-2 (LCN2) in acute liver injury suggest a novel function in liver homeostasis, Biochim Biophys Acta, 2013;1832:660-673.
33. Berard, JL, Zarruk, JG, Arbour, N, et al., Lipocalin 2 is a novel immune mediator of experimental autoimmune encephalomyelitis pathogenesis and is modulated in multiple sclerosis, Glia, 2012;60:1145-1159.
34. Rahman, MS, Murphy, AJ and Woollard, KJ, Effects of dyslipidaemia on monocyte production and function in cardiovascular disease, Nat Rev Cardiol, 2017;14:387-400.

35. Oberoi, R, Bogalle, EP, Matthes, LA, et al., Lipocalin (LCN) 2 Mediates Pro-Atherosclerotic Processes and Is Elevated in Patients with Coronary Artery Disease, PLoS One, 2015;10:e0137924.
36. Warszawska, JM, Gawish, R, Sharif, O, et al., Lipocalin 2 deactivates macrophages and worsens pneumococcal pneumonia outcomes, J Clin Invest, 2013;123:3363-3372.
37. Guo, H, Jin, D and Chen, X, Lipocalin 2 is a regulator of macrophage polarization and NF-kappaB/STAT3 pathway activation, Mol Endocrinol, 2014;28:1616-1628.
38. Nairz, M, Schroll, A, Haschka, D, et al., Lipocalin-2 ensures host defense against Salmonella Typhimurium by controlling macrophage iron homeostasis and immune response, Eur J Immunol, 2015;45:3073-3086.
39. Subbarao, K, Jala, VR, Mathis, S, et al., Role of leukotriene B4 receptors in the development of atherosclerosis: potential mechanisms, Arterioscler Thromb Vasc Biol, 2004;24:369-375.
40. Leskinen, M, Wang, Y, Leszczynski, D, et al., Mast cell chymase induces apoptosis of vascular smooth muscle cells, Arterioscler Thromb Vasc Biol, 2001;21:516-522.
41. Bot, I, de Jager, SC, Zernecke, A, et al., Perivascular mast cells promote atherogenesis and induce plaque destabilization in apolipoprotein E-deficient mice, Circulation, 2007;115:2516-2525.
42. Bot, I, Bot, M, van Heiningen, SH, et al., Mast cell chymase inhibition reduces atherosclerotic plaque progression and improves plaque stability in ApoE-/- mice, Cardiovasc Res, 2011;89:244-252.
43. Giaginis, C, Zira, A, Katsargyris, A, et al., Clinical implication of plasma neutrophil gelatinase-associated lipocalin (NGAL) concentrations in patients with advanced carotid atherosclerosis, Clin Chem Lab Med, 2010;48:1035-1041.

SUPPLEMENTARY FIGURES

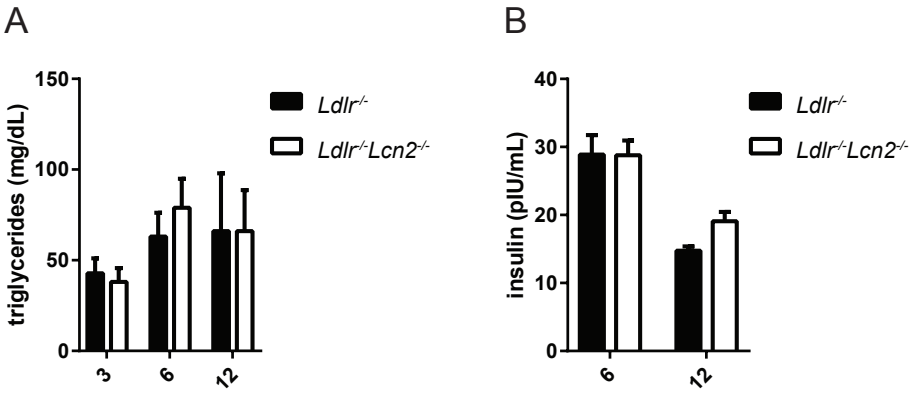

Supplementary figure 1 Triglyceride and insulin concentrations in serum. (A) The levels of triglycerides did not differ between both genotypes after 3, 6 or 12 weeks of WTD. (B) The insulin levels were equal in *Ldlr*$^{-/-}$ mice as compared to *Ldlr*$^{-/-}$*Lcn2*$^{-/-}$ mice after 6 and 12 weeks of WTD. n=10-12 per group.

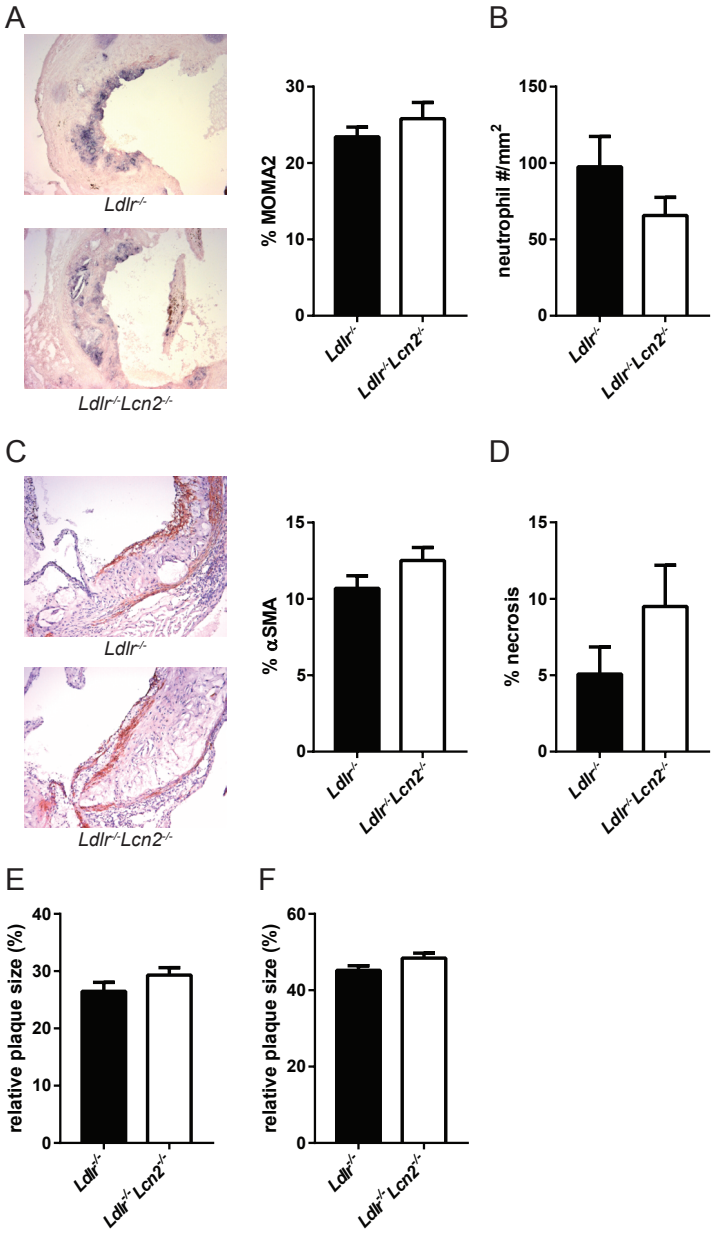

Supplementary figure 2 Plaque composition in 6 weeks and 12 weeks studies (A) Macrophage content as measured by a MOMA2 staining did not differ between groups in advanced lesions. (B) Similarly, total neutrophil numbers was equal between both groups. (C) Also the percentage of smooth muscle cell area inside advanced lesions of *Ldlr*$^{-/-}$ and *Ldlr*$^{-/-}$*Lcn2*$^{-/-}$ was equal between groups. (D) After 6 weeks of WTD, the necrotic core area inside the lesions was equal between both groups. (E) Relative plaque size after 6 weeks WTD was unaltered between both groups. (F) Similarly, after 12 weeks of WTD, relative plaque size in *Ldlr*$^{-/-}$ *Lcn2*$^{-/-}$ mice was equal to *Ldlr*$^{-/-}$ mice. n=12 per group.

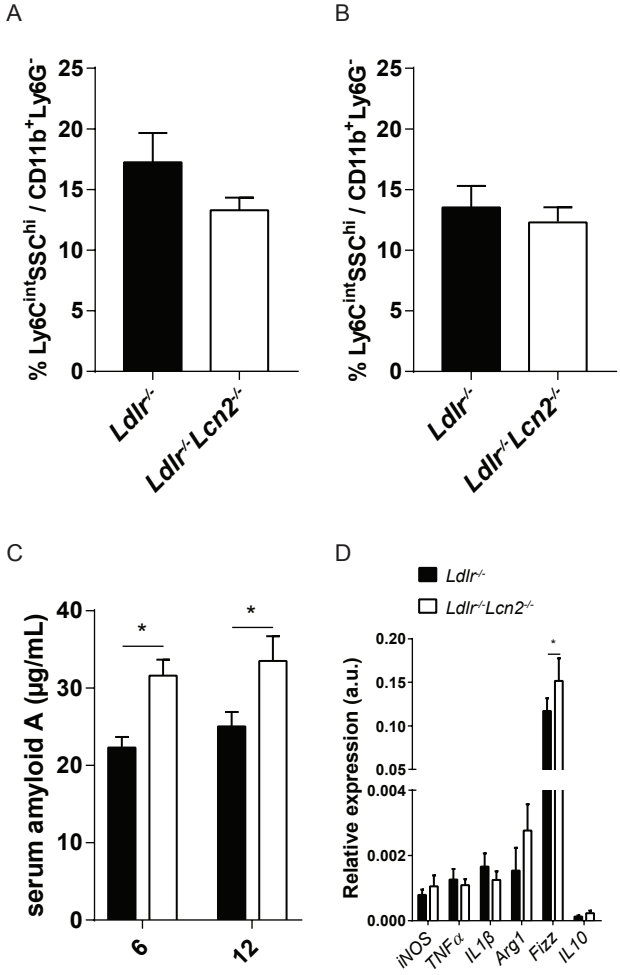

Supplementary figure 3 Assessment of the inflammatory status. (A) No significant changes after 6 weeks of WTD feeding in percentage of eosinophils, as defined as $CD11b^{+}Ly6G^{-}Ly6C^{int}SSC^{hi}$ cells, between both groups was observed. (B) Also after 12 weeks of WTD, no changes were observed in the percentages of eosinophils in the blood. (C) The levels of mouse amyloid A in the serum was higher in *dlr*$^{-/-}$*Lcn2*$^{-/-}$ mice as compared to *Ldlr*$^{-/-}$ mice after both 6 and 12 weeks of WTD. (D) After 6 weeks of WTD, analysis of the expression of M1 and M2 markers in atherosclerotic aortic arches revealed that *Fizz* expression was elevated in *Ldlr*$^{-/-}$*Lcn2*$^{-/-}$ mice. n=6 per group for A, B and D. n=12 for C.

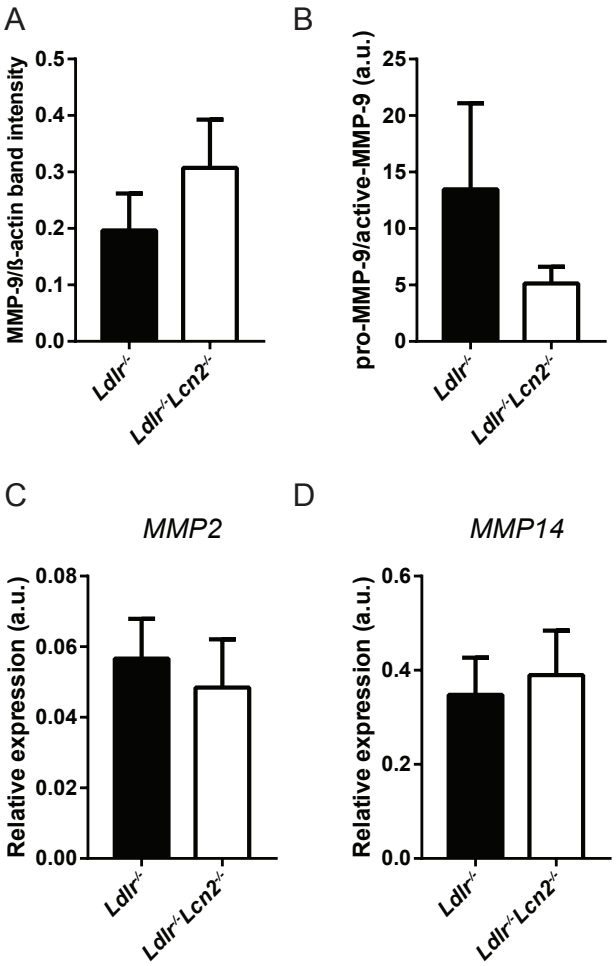

Supplementary Figure 4 MMP expression in atherosclerotic aortic arches. (A) After normalization of MMP-9 protein expression to β-actin protein expression, MMP-9 expression in atherosclerotic aortic arches was equal between *Ldlr*$^{-/-}$*Lcn2*$^{-/-}$ and *Ldlr*$^{-/-}$ mice. (B) The ratio between the pro- and active form of the MMP-9 protein was unaltered between *Ldlr*$^{-/-}$ and *Ldlr*$^{-/-}$*Lcn2*$^{-/-}$ mice. (C) Gene expression of MMP2 in atherosclerotic aortic arches was unaltered in *Ldlr*$^{-/-}$*Lcn2*$^{-/-}$ mice as compared to *Ldlr*$^{-/-}$ mice. (D) Likewise, MMP14 gene expression was equal between both genotypes. n=3 for A-B. n=6 for C and D.

SUPPLEMENTARY TABLES

Supplementary table 1 List of primers used for qPCR expression analysis. Expression of genes were normalized to housekeeping genes *Rpl37* and *Rpl27*.

Gene	Forward primer (5'-3')	Reverse primer (3'-5')
Lcn2	GAACGTTTCACCCGCTTTGCCAAG	GGCAACAGGAAAGATGGAGTGGCAG
24p3r	ctcaatgactctcacggggattgca	aggagaagaggccaaggacagagaa
Arg1	TGGCAGAGGTCCAGAAGAATGG	GTGAGCATCCACCCAAATGACAC
iNOS	TCTGCAGCACTTGGATCAGGAACCT	AGAAACTTCGGAAGGGAGCAATGCC
Fizz	GCCAATCCAGCTAACTATCCCTCCA	CAAGATCCACAGGCAAAGCCACAA
TNFα	GCCTCTTCTCATTCCTGCTTGTG	ATGATCTGAGTGTGAGGGTCTGG
CCL2	CTGAAGCCAGCTCTCTCTTCCTC	GGTGAATGAGTAGCAGCAGGTGA
IL1β	AACGACAAAATACCTGTGGCCTTG	CCGTTTTTCCATCTTCTTCTTTGGGT
MMP2	GATAACCTGGATGCCGTCGTGGA	ACTTCACGCTCTTGAGACTTTGGTTCT
MMP9	CCCTGGAACTCACACGACATCTTC	CTCATTTTGGAAACTCACACGCCAG
MMP14	GGGGTCATTCATGGGCAGTGATGA	GATGATCACCTCCGTCTCCTCCTCA
Rpl37	AGAGACGAAACACTACCGGGACTGG	CTTGGGTTTCGGCGTTGTTCCCTC
Rpl27	CGCCAAGCGATCCAAGATCAAGTCC	AGCTGGGTCCCTGAACACATCCTTG

Supplementary table 2 List of antibodies used for flow cytometry analysis.

Antigen	Fluorochrome	Clone	Manufacterer
CD11b	eFluor 450	M1/70	Ebioscience
Ly6G	FITC	1A8	BD Biosciences
Ly6C	APC	HK1.4	Ebioscience
CXCR2	PE	242216	R&D systems